Mechanism of Heat Transfer in Bubbly Liquid and Liquid-Solid Systems: Single Bubble Injection

Samir Kumar, K. Kusakabe, K. Raghunathan, and L.-S. Fan
Dept. of Chemical Engineering, The Ohio State University, Columbus, OH 43210

Local instantaneous changes in heat-transfer coefficients due to the passage of gas bubbles in liquid and liquid-solid systems are measured. A special heat-transfer probe is developed and located within the bed to trace the instantaneous local heat-transfer rate during the passage of single gas bubbles. A microfoil heat flow sensor is attached to a foil heater, and the sensor-heater probe assembly can accurately measure the heat flux and the surface temperature over a small area. Signals from the sensor are amplified and interfaced with the microcomputer data acquisition system. Simultaneous visualization is performed using a high-speed video camera and a borescope to establish the correspondence between the visual and sensor signals, and hence relate the local instantaneous hydrodynamics to the heat-transfer rate. Local heat-transfer coefficient vs. time traces are analyzed in conjunction with visual signals. The heat-transfer coefficient exhibits a sharp peak in the bubble wake. In both liquid and liquid-solid systems, the observed local maximum in heat-transfer coefficient behind a rising bubble is due to the bubble-wake-induced surface renewal. Enhancement in heat transfer due to the bubble increases with the size because of increased surface renewal caused by larger bubble wake and stronger vortices. The local maximum in heat transfer, however, is more pronounced in liquid than in liquid-solid systems.

Introduction

The gas-liquid-solid fluidized bed has been applied widely to catalytic reactions, biological wastewater treatment and other processes (Fan, 1989). High heat-transfer rate is one of the important characteristics in the operation of a three-phase fluidized bed. The heat-transfer property in the bed is intimately associated with the bubble motion, bubble size, and phase holdup, which are affected by fluid flow including wake flow. The wake flow behavior, such as temporal variations in the shear flow at the bubble edge, chaotic primary wake, and vortex-vortex interaction, differs distinctively from the fluid flow behavior in the bulk region (Fan and Tsuchiya, 1990). To predict fully the heat-transfer performance of gas-liquid and gas-liquid-solid systems, effects of bubble wake need to be considered. The bubble wake effect on heat transfer can be quantified by the measurement of the instantaneous local changes in the heat-transfer coefficient, which depends strongly on the hydrodynamics of the bed.

In three-phase fluidized beds, heat transfer may occur between a particle and the fluid, the liquid and the gas, the wall and the bed, and the bed and internals. Studies on particle-liquid or liquid-gas heat transfer under three-phase fluidization conditions are scarce. Fundamental heat-transfer studies have been concerned mainly with the measurement of time-averaged heat transfer from column wall to the bed and/or from the surface of immersed heating object (rod and cylinder) to bed under steady-state conditions. A comprehensive review was done by Kim and Laurent (1991). Values of heat-transfer coefficient between the bed and the column wall have been reported by Ostergard (1964), Viswanathan et al. (1964), Kato et al. (1981), Chiu and Ziegler (1983), and Muroyama et al. (1984,

Correspondence concerning this article should be addressed to L.-S. Fan.

1986), while those between the surface of the immersed heating object and bed have been reported by Baker et al. (1978), Kato et al. (1984), Kang et al. (1985), and Magiliotou et al. (1988). Heat transfer in gas-liquid-solid systems has a strong dependence on physical properties of the liquid phase and has a weak dependence on gas-phase properties. It is commonly accepted that heat-transfer coefficient increases with gas and liquid velocities, the size and density of the particles, the diameter of the column, and the thermal conductivity and heat capacity of the liquid, but decreases with an increase in liquid viscosity and the diameter of the immersed object (Kim and Laurent, 1991). Baker et al. (1978) reported that the increase in heat-transfer coefficient with gas velocity was initially quite rapid, but became less marked at higher gas flow rates, approaching a maximum value asymptotically. They further reported that the plot of heat-transfer coefficient vs. liquid velocity exhibited a maximum, similar to that observed in liquid-solid fluidized beds. The bed voidage at which the maximum heat transfer occurred decreased with particle size, but increased with liquid viscosity (Kang et al., 1985). Chiu and Ziegler (1983) reported higher heat transfer from wall to bed in a three-phase fluidized bed compared to that in liquid-solid and gas-liquid systems except under the condition of small particles and high gas velocities. They postulated that the product of the heat-transfer coefficient and the liquid holdup remains the same in liquid-solid and gas-liquid-solid systems and proposed a model based on the thermal resistance of the bed. Deckwer (1980) proposed a heat-transfer mechanism in bubble columns based on Higbie's surface renewal theory combined with Kolmogoroff's theory of isotropic turbulence. Several other investigators (Suh et al., 1985; Magiliotou et al., 1988; Suh and Deckwer, 1989) extended this concept to three-phase fluidized beds by modifying the energy dissipation rate to include the increased surface renewal due to increased turbulence created by solid particles. Suh et al. (1985) and Suh and Deckwer (1989) neglected the effect of particle convective transport on the heat transfer, while Magiliotou et al. (1988) proposed that particles also contribute to heat transfer in both liquid-solid and gas-liquid-solid fluidized beds in conjunction with isotropic fluid microeddies. Being semitheoretical in approach, these studies do not fully reflect the inherent mechanism underlying the heat transfer in three-phase fluidized beds.

Presently, little data are available for the instantaneous changes in heat-transfer coefficient due to variation in bubble motion and bubble size in such systems. While much progress has been made in the understanding of immersed object to bed and wall to bed heat transfer, precise bubble wake effect on heat transfer remains unexplored. Kubie (1975) reported bubble-induced heat transfer in two-phase gas-liquid flow. In his study, two-phase flow was simulated by generating a single continuous stream of discrete gas bubbles into a stationary liquid. From his experiments, he predicted bubble wake to be responsible primarily for heat-transfer enhancement. Arters et al. (1989) measured instantaneous changes in liquid-solid mass-transfer coefficient for a single particle in the wake region behind a single bubble in a liquid-solid fluidized bed. In their study, the instantaneous mass-transfer coefficients were determined by using electrochemical methods, and visualization technique was employed simultaneously to track the particle in relation to bubble and bubble wake. They reported that the enhancement of mass-transfer coefficient takes place in the wake. Raghunathan et al. (1992) studied the pressure distribution and vortical structure in the wake behind single gas bubbles in stagnant water and 163-μm and 326-μm glass-beads fluidized bed. They reported significant effect of solids on primary wake flow behavior. Thus, a fundamental understanding of bubble wake dynamics forms a necessary basis for a complete description of various transport processes in these systems.

The wake phenomena were summarized recently by Fan and Tsuchiya (1990). It is commonly accepted that gas-phase-induced turbulence is responsible for the high heat-transfer rate in three-phase systems. The turbulence lies in the regions of the bubble wake with shear and turbulent flows, the free shear layer at the bubble edge, the chaotic primary wake, vortices shed or in the process of shedding from the primary wake, and in areas of vortex-vortex interaction.

In the present study, specific effects of the bubble wake on the heat-transfer characteristics are investigated by measuring local instantaneous changes in heat-transfer rate due to the passage of a single gas bubble in liquid and liquid-solid systems. A special heat-transfer probe is developed which is used to measure instantaneous local heat-transfer coefficients after a single gas bubble is injected in liquid and liquid-solid systems. Simultaneous visualization is performed to ascertain the role of bubble and bubble wake in the enhancement of heat transfer. The visualization examines the liquid flow pattern and local solids motion due to the bubble-induced turbulence in liquid and liquid-solid systems, respectively.

Experimental Studies

A schematic diagram of the experimental apparatus is shown in Figure 1. The experiments are performed in a three-dimensional Plexiglas column, 150 cm high and 7.62 cm ID. Liquid

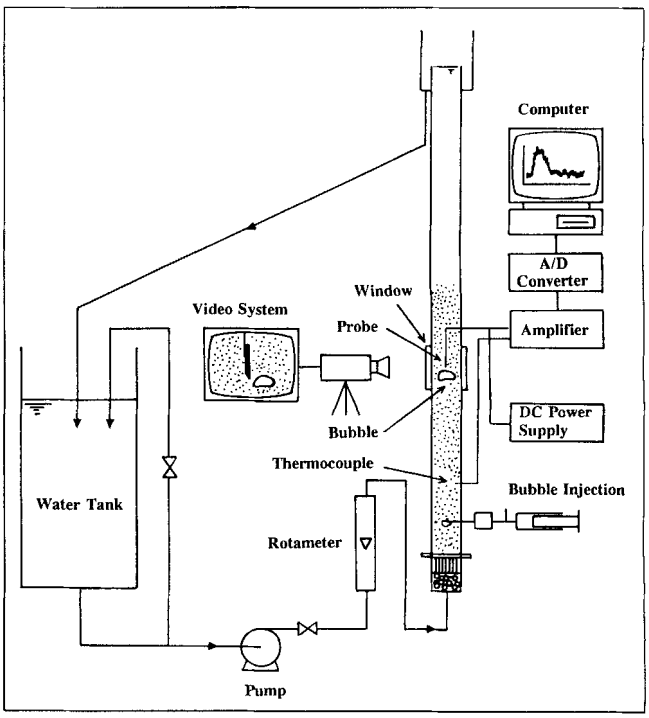

Figure 1. Experimental setup.

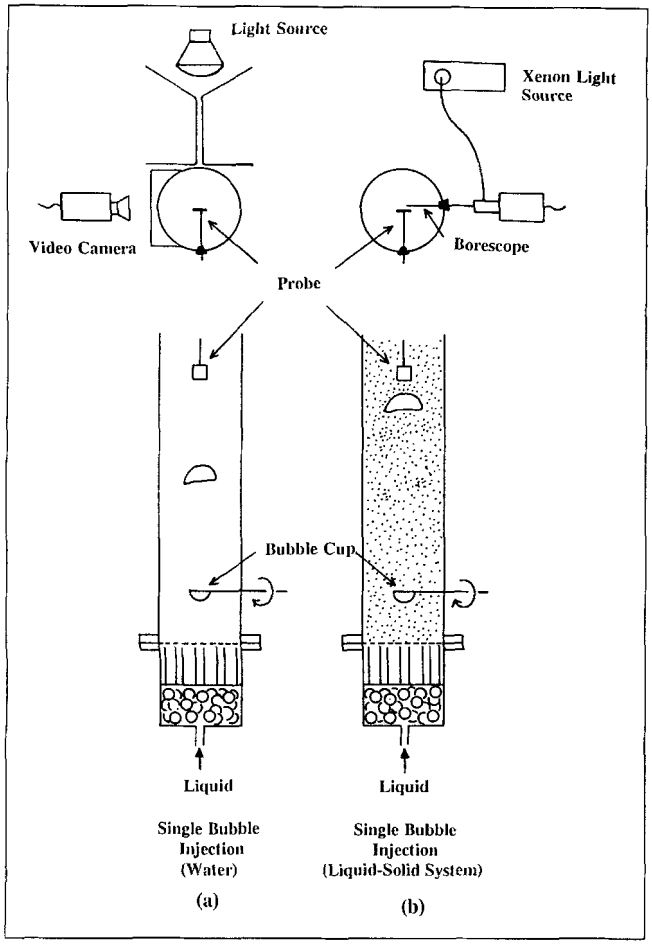

Figure 2. Experimental conditions.

enters the column through a packed layer of 6-mm glass beads and a perforated-plate distributor ensuring uniform distribution of liquid in the column. The support for the fluidized particles is provided by 200-mesh wire cloth. A steady liquid velocity is maintained by circulating water through a reservoir and a rotary pump.

Experiments involve single bubble injection in liquids and liquid-solid suspensions as shown in Figures 2a and 2b. A three-dimensional cup bubble injection system in Figure 1 is designed in this study to introduce single bubbles without pressure perturbation or any satellites generation. Hemispherical cup of 2.5 cm diameter is inserted through the wall at 10 cm above the distributor. A known volume of air is injected into the cup through the stainless tube using a syringe. The trapped bubble is then released by turning the cup. Tap water is used as the liquid phase in the experiments. Fluidized particles used are 163-μm (GB163) and 326-μm (GB326) glass beads. The physical properties of solid particles are given in Table 1. The bubble volume varied from 3 cm^3 to 10 cm^3 with the corresponding bubble Reynolds number (based on equivalent bubble diameter) *Re* ranging from 4,600 to 7,700. Under these values of *Re*, the bubble is of spherical cap shape, and the wake configuration is symmetric along the vertical axis of bubble. Furthermore, the bubbles rose almost rectilinearly. Miyahara et al. (1988) reported that for *Re* beyond 5,000 the bubble tends to discharge vorticity symmetrically and rises rectilinearly.

Table 1. Physical Properties of Spherical Particles

Particle	Notation	Avg. Dia. (mm)	Density (g/cm^3)	ϵ_{s0}^*	U_t^{**} (m/s)
Glass Bead	GB163	0.163	2.50	0.63	1.7×10^{-2}
Glass Bead	GB326	0.326	2.50	0.62	4.4×10^{-2}

* Packed bed solids fraction
**Fan and Tsuchiya (1990)

Instantaneous heat-transfer measurement

The instantaneous local heat-transfer rate is measured by a heat flow sensor/heater assembly (heat transfer probe). Figure 3 shows the details of the probe design. The probe assembly consists of five components: microfoil heat-flow sensor, copper plate, foil heater, thermosetting material (insulator), and support. The foil heater is 2.54 cm high and 1.91 cm wide, and is heated by a constant voltage DC power source.

The local heat flux is measured directly by a microfoil differential heat-flow sensor (RdF corporation, Model 20453-1). The overall dimension of the sensor is 1.27 cm $\times$ 1.27 cm $\times$ 0.008 cm. This sensor utilizes thin-foil-type thermopiles bonded to both sides of a known thermal barrier. The difference in temperature across the thermal barrier is proportional to heat flow through the sensor. With the dimensions of the thermal barrier known, the sensor is factory-calibrated to provide the relation between sensor output (voltage) and the local heat flux. The unique construction of the sensor provides it with low thermal capacitance (204.41 $J\cdot m^{-2}/K$), low thermal impedance (5.28×10^{-4} $m^2\cdot K/W$), high sensitivity (8.56×10^{-3} $\mu V/W\cdot m^{-2}$), fast response time (0.02 s), and minimal thermal perturbation to the heat flow. The microfoil heat flow sensor is flush mounted on the copper plate which is attached to the micro-foil heater and insulator as shown in Figure 3. The sensor can accurately measure the heat flux and its surface temperature over a small surface area. The heater/sensor probe assembly is usually positioned in the center of column with the help of a support as shown in Figure 1. Due to the rectilinear motion of bubble, there is a high probability of bubble striking the probe surface or at least passing very close to it. The probe is located at about 50 cm from the point of bubble injection, which allows sufficient distance for the bubble to reach its terminal velocity (Miyahara et al., 1988). Since the width of

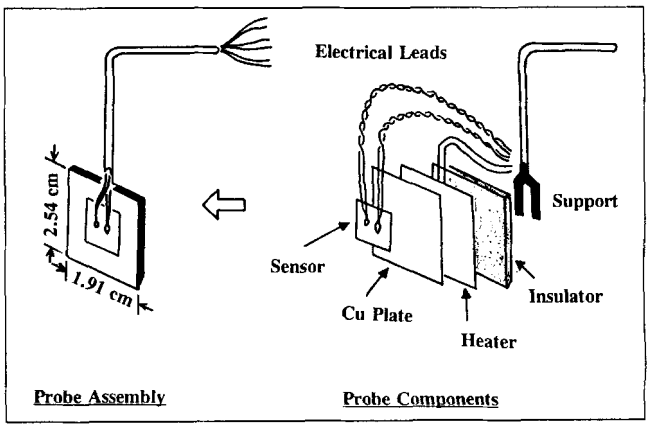

Figure 3. Heat-transfer probe design.

the probe at a horizontal section of the column is small (0.32 cm), the disturbance to the flow in the vicinity of the probe is minimal and the fluidized state remains relatively undisturbed. A sheathed copper-constantan thermocouple located at the column wall is used for measurement of the bulk temperature. The average bulk temperature is also monitored by a digital thermometer.

Signals for the heat flux as well as the temperature difference between probe surface and bulk are sampled simultaneously at the rate of 186.2 Hz for 11 seconds. The signals from the sensor (typically in microvolts range) are amplified to millivolts range by the amplifier/multiplexer system (Metrabyte EXP-16) and interfaced with the high-speed microcomputer data acquisition system (Metrabyte DASH-16). Digital signals stored in the computer are converted to the corresponding heat-transfer rate and the temperature difference using proper calibration. To reduce the high-frequency noise in the original signal, software signal processing is performed. The signals are smoothed by employing a low-pass filter and the computations are done using Fast Fourier Transforms. A typical raw and filtered signal of the temperature difference ΔT_i $(=T_{si}-T_\infty)$ for a single bubble injection in liquid-solid fluidized bed containing GB163 is shown in Figure 4. There is a significant change in temperature difference due to the passage of bubble, but the change in q_i is not so significant compared to the temperature difference. Also, there is a large fluctuation in q_i as compared to ΔT_i. Since the change in the instantaneous heat-transfer rate depends on many factors including the thermal balance on both sides of heater, the instantaneous heat-transfer coefficient, h_i, is obtained from the instantaneous change in the temperature difference, ΔT_i, and the time averaged heat-transfer rate, Q.

$$h_i = Q/\Delta T_i \tag{1}$$

Visualization

Experiments are performed to investigate the wake effect of a single gas bubble on instantaneous heat transfer in liquid system as shown in Figure 1 and Figure 2a. The liquid flow pattern in the vicinity of heat-transfer probe is visualized using plyolite particles ($\rho_p = 1.024$ g/cm^3, $d_p = 250$–380 μm) as the liquid flow tracer. The test section is enclosed in a rectangular viewing vessel made of Plexiglas and filled with tap water (shown in Figure 1) to minimize optical distortion. Lighting is applied from the side through a slit to provide a narrow vertical light sheet normal to the probe surface to obtain a two-dimensional view of the wake flow in the vicinity of probe. The wake structure is observed by a stationary high-speed video camera (Pulnix) focused in the direction normal to the sheet of light. The video camera is synchronized with the data acquisition system. The signals from the camera are stored by a video recorder (Sony VO-5800 U-matic) at a rate of 60 frames/s. A light-emitting diode (LED) is located at the front wall of the column in the view of the video camera. An external trigger activates the data acquisition system and illuminates the LED simultaneously. Thus, precise synchronization of the video and heat-transfer signals is achieved.

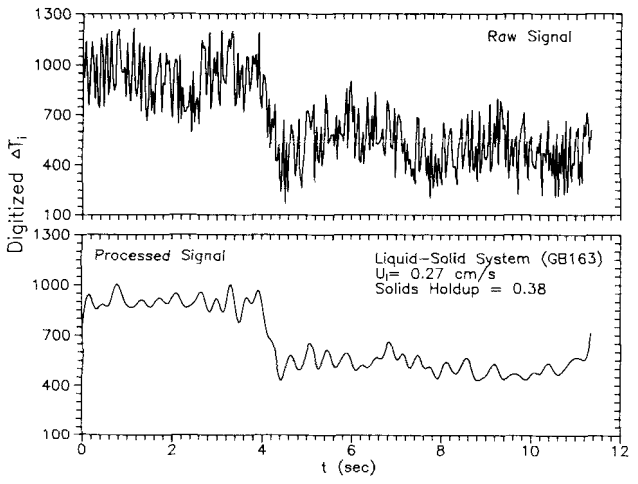

Figure 4. Typical raw and processed signal.

Heat-transfer experiments with single bubble injection in the liquid-solid system containing GB163 ($\epsilon_l = 0.98$) are synchronized with *in-situ* visualization to study the effects of local solids motion. Simultaneous *in-situ* visualization is performed using a borescope (Olympus K-17-18-0062) as shown in Figure 2b to establish relationships between the visual and sensor signals. The borescope is interfaced with the high-speed video camera (Pulnix), and the visual signals from the camera are stored by the video recorder. The tip of the borescope is placed close to the sensor surface as shown in Figure 2b. Thus, only the solid particles close to the sensor surface are in focus and can be seen on the video screen. Light is provided by a Xenon high-intensity light source and is transmitted to the tip of borescope through an optic-fiber cable.

Results and Discussion

A frame-by-frame analysis of video signals is performed in conjunction with the heat-transfer signals to investigate the effect of bubble wake on instantaneous local heat-transfer coefficients. For stationary water, a representative heat-transfer signal and selected photographs of the liquid flow pattern due to the passage of bubble corresponding to this signal are shown in Figures 5a and 5b, respectively. The photographs in Figure 5b are marked according to the corresponding points on the heat-transfer signal. White dots are the plyolite tracer particles, and the white vertical object is the heat-transfer probe. The dark portion behind the probe is due to the shadow of the probe. The streak of tracer particles following the liquid flow can be observed. The tip of the arrow indicates the location of the heat-transfer sensor. In this run, the probe is located at the center of column and the injected bubble volume is 3 cm^3. The instantaneous heat-transfer coefficient begins to increase as the bubble approaches the lower edge of the heat-transfer probe assembly (photograph A in Figure 5b). This is due to the surface renewal caused by the liquid being pushed by the bubble. The approaching bubble forces the heated liquid at the probe away from the probe and partially renews it with the cooler liquid from the bulk.

When the gas bubble is in the vicinity of sensor (photograph B in Figure 5b), the instantaneous heat-transfer coefficient is still increasing due to increased renewal caused by the bubble. The projection of the three-dimensional vortex structure appears in the plane of visualization as a pair of vortices. The structure of the wake appears to be symmetric about the vertical

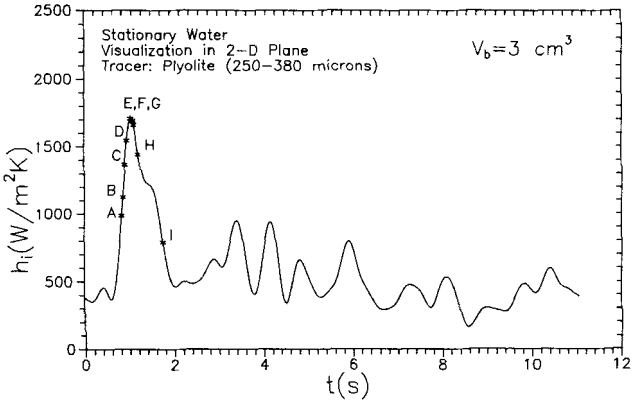

(a) Experimental Data

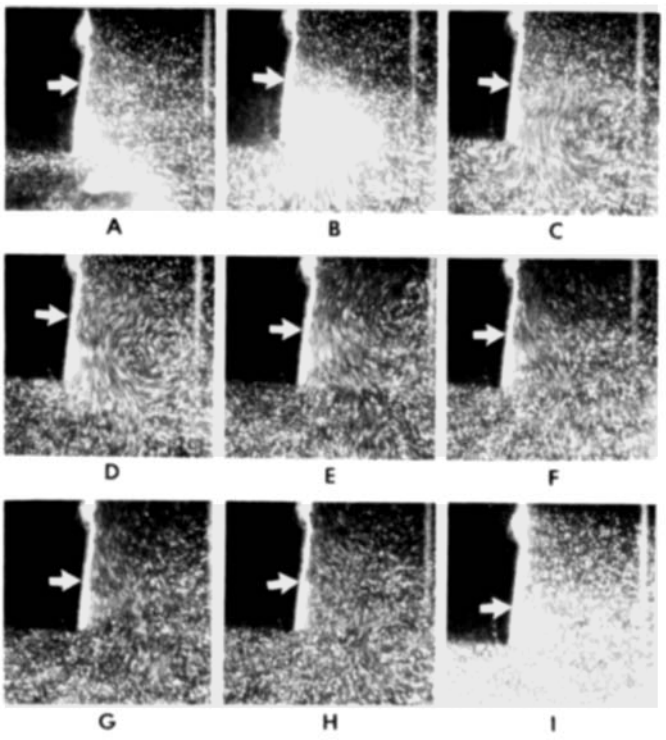

(b) Visualization

Figure 5. Instantaneous heat-transfer data synchronized with visualization for probe located at the center of column.

axis of the bubble movement, and the bubble is of spherical cap shape.

In photographs C and D, the bubble has disappeared behind the illuminated two-dimensional plane. The vortex size, however, increases in the primary wake and thus increased heat-transfer coefficient is obtained. As the bubble passes close to the probe surface, the heated liquid at the surface is being continuously replaced by the cold liquid brought by the passing bubble in its wake.

The maximum instantaneous heat-transfer coefficients are obtained in the wake region (photographs E, F and G) due to strong liquid circulation caused by the wake that induces rapid surface renewal. In the two-dimensional plane of visualization, the probe surface appears to lie in the middle of the vortex structure and thus experiences high shear flow due to induced liquid flow toward the wake central axis. The vortex entrains fluid from around the wake and induces rapid surface renewal. The probe surface is lying close to the wake central axis, and the liquid flow is upward near the wake central axis. The absolute upward velocity of the fluid element in the vicinity of the probe could be calculated by following a tracer particle in successive video frames. The absolute upward velocity is in the range of 25 cm/s, which is the same as the measured bubble rise velocity.

Photograph H shows a shedded vortex renewing the heat-transfer surface. The strength of turbulence created by the bubble wake is diminished due to the viscous dissipation of vorticity, resulting in decreased heat transfer.

Photograph I shows no bubble in the vicinity of probe surface; however, the probe surface still interacts with the secondary wake, and the turbulence in the medium can be observed by the streak of tracer particles.

From this and similar experimental runs it is evident that the maxima in heat-transfer signals correspond to the maximum local turbulence created by the bubble wake. The maximum heat transfer is obtained in the region of high shear flows. The region of high shear flows exists in the upward flow along the wake central axis behind the bubble. The mechanism behind a substantial increase in the heat-transfer coefficient due to the interaction with bubble wake may be twofold. High shear flow in the wake region may decrease the thickness of the thermal boundary layer on the probe surface causing increased heat transfer. This effect is coupled with the rapid surface renewal induced entrainment of fluid from around the wake by the vortex. Arters et al. (1989) also observed substantial increase in the particle-liquid mass-transfer coefficient when a particle interacts with wake region. They reported that the increase may take place at quite a distance from the bubble, but it always occurred in regions of high shear flow, such as that occurring between two shed vortices or in the cross flow between the primary wake and shed vortices. In their study, the largest increases in mass transfer occurred usually between two vortices in the high shear flow region associated with crossing over behind the bubble.

Figure 6 shows the heat-transfer signal for probe located near the wall. This signal is also analyzed in conjunction with the video pictures. Corresponding photographs for the points marked in the signal also are shown. In this signal, increase and decrease in heat-transfer coefficient are gradual due primarily to lower turbulence sensed by the probe. The maximum in the signal is observed much after the bubble has passed from the view of the camera. The maxima in this signal are due apparently to the shedded wake interacting with probe surface.

Results for the probe located near the wall indicate that the bubble-wake-induced enhancement depends on lateral distance from the bubble rise path. Enhancement in heat transfer due to the passage of bubble in this case is much smaller than the case where the probe is located at the center of column (Figure 5a). Arters et al. (1989) also reported lesser increases in mass transfer for particles skirting the edge of the wake region without being drawn in and for those lying outside the wake. Nevertheless, the enhancement is still caused by the bubble wake.

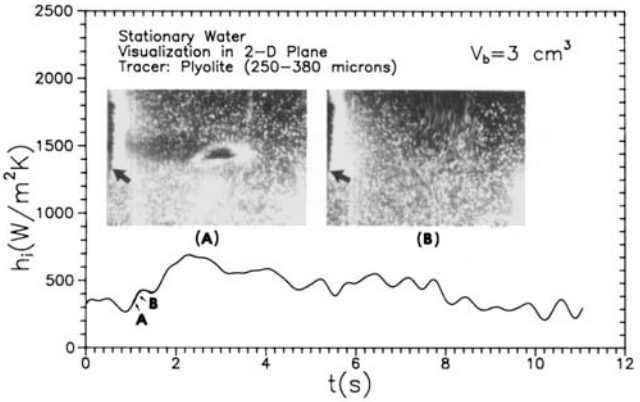

Figure 6. Instantaneous heat-transfer data synchronized with visualization for probe located in the vicinity of wall.

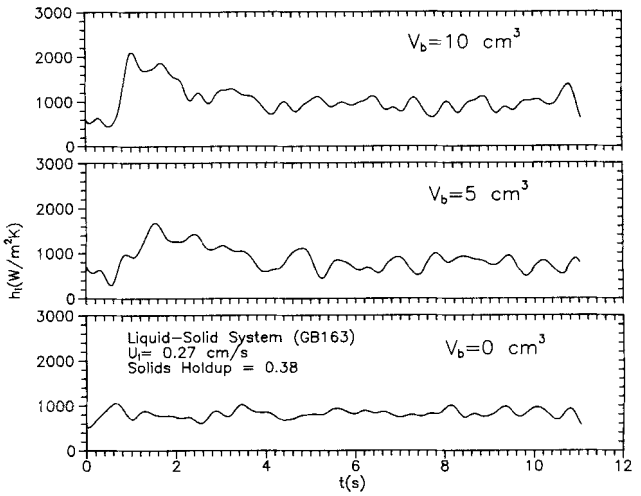

Figure 8. Effects of bubble size on instantaneous heat-transfer coefficient due to the passage of bubble in liquid-solid fluidized bed with GB163 for probe located at the center of column.

Instantaneous heat-transfer coefficient

Figures 7, 8 and 9 show the instantaneous heat-transfer coefficient due to the passage of a single gas bubble in liquid, in liquid-solid system containing GB163, and in liquid-solid system containing GB326, respectively. The instantaneous heat-transfer coefficient increased rapidly, attained a maximum value, and then gradually recovered to the initial value in liquid and liquid-solid systems. It should also be noted from Figures 7, 8 and 9 that due to the presence of secondary wake in liquid and liquid-solid systems, the heat-transfer coefficient does not completely recover to the baseline value within the sampling time of around 11 s. The effect of single bubble injection on heat-transfer enhancement in the liquid system lasts much longer than liquid-solid systems. Larger primary and secondary wakes and stronger vortex in such systems are responsible primarily for this phenomenon. Considerably more fluctuations are observed in the liquid-solid system than in the liquid system. This is due apparently to the local turbulence created by the particle and its wake. All these figures show that increased bubble volume V_b causes increased enhancement due to larger bubble wake and stronger vortices. Miyahara et al. (1988) reported that the mean ratio of the primary wake size to the bubble size is almost independent of Re and had a mean value of around 4.7 for symmetric wake configuration. Thus, a larger bubble would have a larger wake and stronger vortices, which would induce greater turbulence and hence increased surface renewal compared to a smaller bubble wake.

Particle sizes in liquid-solid systems affect the bubble-wake-induced heat-transfer enhancement. Disturbance caused in the heat-transfer signal due to the particle-induced local turbulence is significantly higher in the liquid-solid system containing

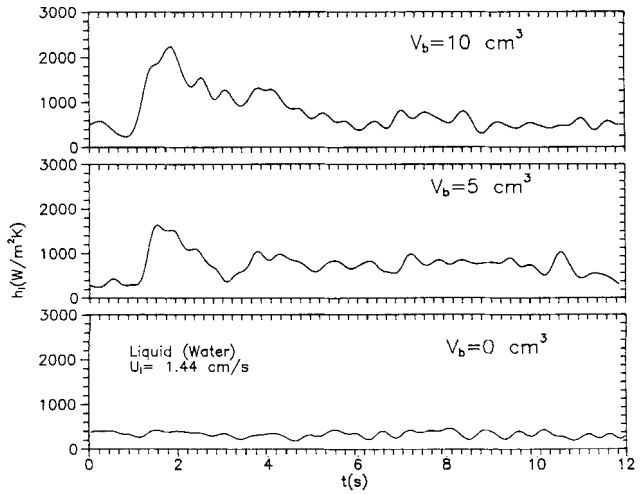

Figure 7. Effects of bubble size on instantaneous heat-transfer coefficient due to the passage of bubble in liquid for probe located at the center of column.

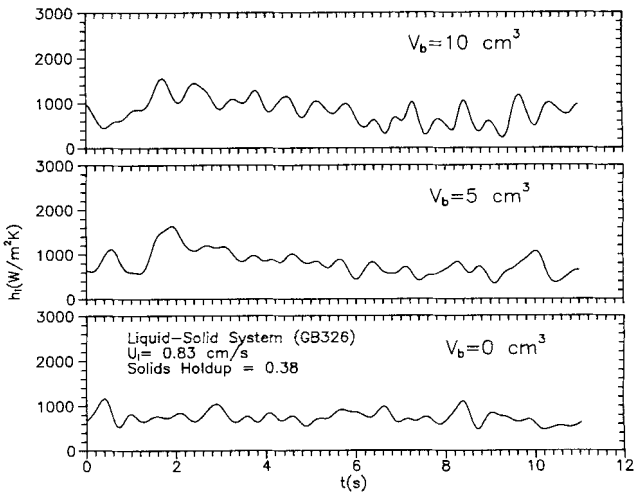

Figure 9. Effects of bubble size on instantaneous heat-transfer coefficient due to the passage of bubble in liquid-solid fluidized bed with GB326 for probe located at the center of column.

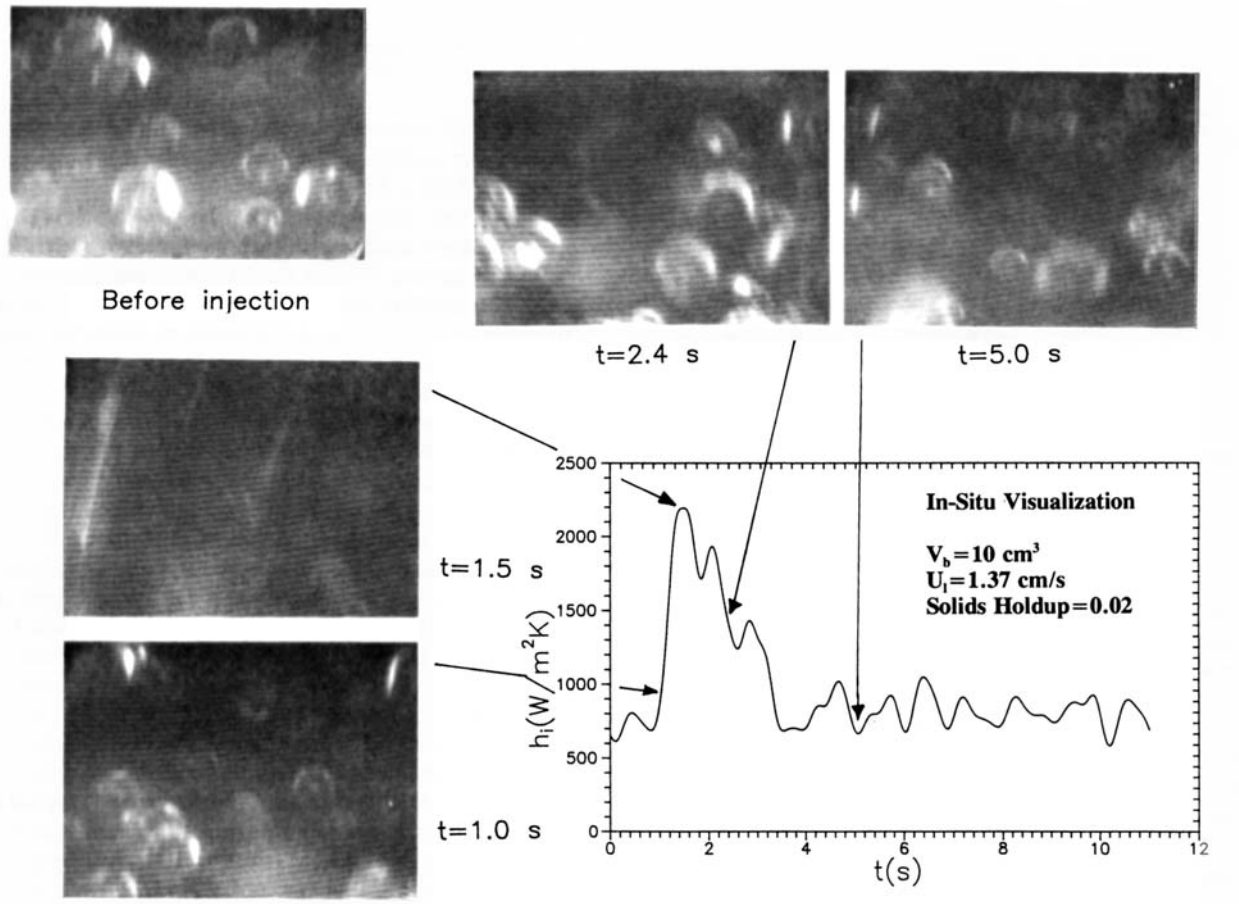

Figure 10. Instantaneous heat-transfer signal synchronized with visualization using borescope for single bubble passage in liquid-solid fluidized bed.

GB326 (Figure 9) than that for GB163 (Figure 8). Heterogenous effects caused by the larger particle size reduce the bubble-wake-induced enhancement in heat transfer although the baseline value is increased. Note that for the liquid-solid system containing GB326, heterogenous effects caused by the particle in the system destroy ordered motion/circulation resulting in reduced vortical strength compared with that in water and liquid-solid systems containing GB163 (Raghunathan et al., 1992). The baseline values (time-averaged heat-transfer coefficient with no bubble injection) for liquid is 285 W/m²•K, for GB163 system is 808 W/m²•K, and for GB326 system is 815 W/m²•K.

Figure 10 shows the *in-situ* visualization of local solids motion in the vicinity of the probe due to the passage of single gas bubble in the liquid-solid fluidized bed containing GB163. These photographs are again analyzed in conjunction with the heat-transfer signal. The photographs of local solids motion before the injection of bubble and at different times after the injection are shown in Figure 10. The maximum in the heat-transfer signal is observed at $t=1.5$ s; at $t=1.5$ s, the streak of light shows that the particles are moving much faster, making it difficult to observe them. The average upward velocity of solid particles is calculated by measuring the distance traveled by a single particle in three consecutive frames (1/20 s). Particles at this particular instant are moving at 26 cm/s, which is approximately equal to the bubble rise velocity. This indicates that the particles are apparently in the wake region and the maximum heat transfer is obtained in the bubble wake which is in accordance with that in stationary water. Before the injection of bubble, the local solids motion is random as shown in this figure. The sharp boundary of solid particles indicates that particles are moving slowly. Due to the random nature of solids motion, there are no significant differences for $t=1.0$ s, 2.4 s and 5.0 s. In the video frame at $t=2.4$ s, however, the particles are moving relatively faster than those at $t=1.0$ s and 5.0 s.

Figure 11 compares relative enhancement in heat transfer in various systems made by time-averaging the heat-transfer signal. The time-averaged heat-transfer coefficient is obtained by:

$$\bar{h}_i=\frac{1}{(t_f-t_i)}\int_{t_i}^{t_f} h_i dt \qquad (2)$$

where t_i corresponds to the time in the signal where the heat transfer starts increasing due to the effect of oncoming bubble and t_f corresponds to the upper limit for averaging. In our

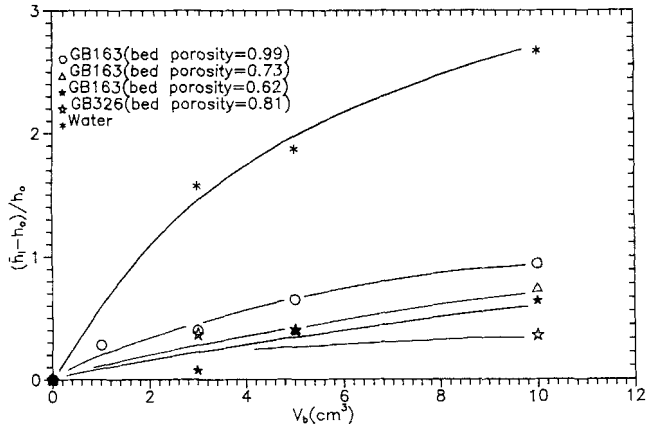

Figure 11. Comparison of heat-transfer enhancement due to single bubble passage in different systems.

calculation, $(t_f - t_i)$ is set at 4 s, by which time bubble has already left the column. It turns out that for averaging time over 4 s, this duration has little effect on the trends shown in the figure. Although the time-averaged heat-transfer coefficient in the liquid-solid fluidized bed is higher than that in liquid, the enhancement in instantaneous heat-transfer coefficient due to the passage of single bubble is relatively more pronounced in the liquid system than that in the liquid-solid fluidized bed. Heat-transfer enhancement due to single bubble passage increases with increased bed expansion because of larger bubble wake and increased vortical strength. At higher solids holdup, the heterogenous effects in GB163, that is, small-scale disturbances caused by random motion of solid particles and their wake, reduce the apparent strength of vortical flow and thus reduce the surface renewal caused by the bubble wake at the probe surface. It is also interesting to note that for GB163 bed with bed porosity = 0.99, the heat-transfer enhancement differs markedly from that in water.

Modeling

The mechanism of heat-transfer enhancement due to the passage of a gas bubble could be explained by consecutive film and surface renewal theory proposed by Wasan and Ahluwalia (1969). Such a theory can predict heat exchange between a flat plate and a fluid flowing parallel to it. In this model a thin film of uniform thickness, δ, is viewed to lie at the probe surface, and a mass of fluid brought by the bubble wake is viewed to exchange heat by unsteady-state conduction at the outer edge of the film. The renewal of fluid on the probe surface is caused by the bubble wake and the temperature of the fluid element sweeping the outer surface of the film is assumed to be uniform and equal to the bulk fluid temperature, T_∞. The temperature of the interface between the film and fluid element changes with time and instantaneous heat-transfer rate to the fluid element is defined assuming no heat storage in the film. Based on these assumptions, Wasan and Ahluwalia (1969) proposed the following relationship for the average of instantaneous heat-transfer coefficient over the contact time, t_c:

$$h_{av} = \frac{2k}{\sqrt{(\pi\alpha t_c)}} + \frac{k\delta}{\alpha t_c}\left[e^{\frac{\alpha t_c}{\delta^2}}\left(1 - erf\frac{\sqrt{(\alpha t_c)}}{\delta}\right) - 1\right] \qquad (3)$$

Each fluid element brought by the bubble in its wake stays at the outer surface of the film for a contact time, t_c, until it is replaced by a fresh fluid element, which in turn is later washed away. As mentioned earlier, the maximum in heat-transfer rate is observed in the region of high shear flow, that is, in the upward flow of fluid rising along the wake central axis. The absolute velocity of the fluid elements rising along the wake central axis can be calculated by following the plyolite tracer particles in successive video frames. It is observed that the absolute upward velocity of the fluid element along the wake central axis is equal to the bubble rise velocity. Fan and Tsuchiya (1990) reported that the particle velocity relative to the bubble along the wake central axis in the region covering the cross flow is zero. Hence, a reasonable estimate of contact time could be obtained from the absolute bubble rise velocity.

Figure 12 shows a comparison of actual heat-transfer enhancement in stagnant water with the average heat transfer predicted by this model. It is assumed that between $t = 0.65$ s and $t = 2.0$ s in the heat-transfer signal, each fluid element brought by the bubble in its wake stays at the outer surface of the film for contact time t_c $(= L/U_b)$. The film thickness is calculated based on natural convection in the medium and is assumed to be constant during this period. The film thickness is equal to the thickness of a natural convection thermal boundary layer and is approximately equal to 0.5 mm. The predicted heat-transfer coefficient h_{av} is within 10% of the experimental time-averaged heat-transfer coefficient h'_{av}. The model is reasonably accurate and provides a mechanistic insight into the heat-transfer enhancement due to a bubble.

Conclusions

A heat-transfer probe is developed which accurately measured the instantaneous changes in heat transfer due to the passage of single gas bubble in liquid and liquid-solid systems. Simultaneous visualization is performed, and specific effects of bubble wake on heat-transfer enhancement are identified.

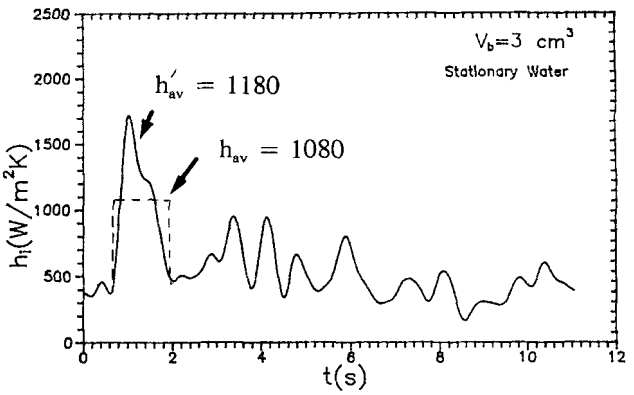

Figure 12. Comparison of model-predicted time-averaged heat-transfer coefficient with experimental time-averaged heat-transfer coefficient.

For a bubble passing through the probe, the maximum heat transfer is observed in the wake region at a short distance behind the bubble in the upward flow of fluid rising along the wake central axis. For a bubble passing away from the probe surface, the maximum heat transfer is obtained at a much larger distance behind the bubble and is apparently due to the interaction with a shedded wake.

Bubble size, particle size, and solids holdup in the bed affect the bubble-wake-induced heat-transfer enhancement. Enhancement is relatively more pronounced in the liquid system than in liquid-solid systems, although the baseline heat-transfer coefficient values for liquid-solid systems are higher than those in the liquid system.

The maximum heat transfer in liquid and liquid-solid systems due to the passage of single gas bubble is obtained in the bubble wake in the region of high shear flows. Bubble wake is responsible primarily for the rapid surface renewal of fluid on the probe surface resulting in enhanced heat transfer. The magnitude of the average heat-transfer enhancement is well predicted by consecutive film and surface renewal theory.

Acknowledgment

This work was supported by NSF Grant # CTS-8905463.

Notation

d_p = particle diameter, μm
h_{av} = average heat-transfer coefficient over t_c, W/m^2•K
h'_{av} = time-averaged experimental heat-transfer coefficient, W/m^2•K
h_i = instantaneous heat-transfer coefficient, W/m^2•K
$\bar{h}_i$ = time-averaged heat-transfer coefficient over 4 s, W/m^2•K
h_o = baseline heat-transfer coefficient without bubble, W/m^2•K
k = thermal conductivity, W/m•K
L = length of the microfoil heat flow sensor, cm
q_i = instantaneous heat flux, W/m^2
Q = time-averaged heat flux, W/m^2
t = real time, s
t_c = contact time, s
t_f = time corresponding to the upper limit for averaging h_i, s
t_i = time corresponding to the lower limit for averaging h_i, s
T_{si} = instantaneous probe surface temperature, K
T_∞ = bulk temperature, K
U_b = absolute bubble rise velocity, cm/s
U_l = superficial liquid velocity, cm/s
U_t = particle terminal velocity, cm/s
V_b = bubble volume, cm^3

Greek letters

α = thermal diffusivity, cm^2/s
δ = average film thickness, cm
ΔT_i = instantaneous temperature difference between probe surface and bulk, K
ϵ_l = bed porosity
ϵ_{s0} = packed-bed solids fraction
ρ_p = particle density, g/cm^3

Literature Cited

Arters, D. C., K. Tsuchiya, and L.-S. Fan, "Solid-Liquid Mass Transfer in the Wake Region behind a Single Bubble in a Liquid-Solid Fluidized Bed," *Fluidization VI*, p. 507, J. R. Grace, L. W. Shemilt, and M. A. Bergougnou, eds., Engineering Foundation, New York (1989).

Baker, C. G. J., E. R. Armstrong, and M. A. Bergougnou, "Heat Transfer in Three-Phase Fluidized Beds," *Powder Technol.*, **21**, 195 (1978).

Chiu, T. M., and E. N. Ziegler, "Heat Transfer in Three-Phase Fluidized Beds," *AIChE J.*, **29**(4), 677 (1983).

Deckwer, W.-D., "On the Mechanism of Heat Transfer in Bubble Column Reactors," *Chem. Eng. Sci.*, **35**, 1341 (1980).

Fan, L.-S., *Gas-Liquid-Solid Fluidization Engineering*, Butterworths, Stoneham, MA (1989).

Fan, L.-S., and K. Tsuchiya, *Bubble Wake Dynamics in Liquids and Liquid-Solid Suspensions*, Butterworth-Heinemann, Stoneham, MA (1990).

Kang, Y., I. S. Suh, and S. D. Kim, "Heat Transfer Characteristics of Three Phase Fluidized Beds," *Chem. Eng. Commun.*, **34**, 1 (1985).

Kato, Y., K. Uchida, T. Kago, and S. Morooka, "Liquid Holdup and Heat-Transfer Coefficient between Bed and Wall in Liquid-Solid and Gas-Liquid-Solid Fluidized Beds," *Powder Technol.*, **28**, 173 (1981).

Kato, Y., Y. Taura, T. Kago, and S. Morooka, "Heat Transfer Coefficient Between an Inserted Vertical Tube and a Three-Phase Fluidized Bed," *Kagaku Kogaku Ronbunshu*, **10**, 427 (1984).

Kim, S. D., and A. Laurent, "The State of Knowledge on Heat Transfer in Three-Phase Fluidized Beds," *Int. Chem. Eng.*, **31**, 284 (1991).

Kubie, J., "Bubble Induced Heat Transfer in Two Phase Gas-Liquid Flow," *Int. J. Heat Mass Transfer*, **18**, 537 (1975).

Magiliotou, M., Y.-M. Chen, and L.-S. Fan, "Bed-Immersed Object Heat Transfer in a Three-Phase Fluidized Bed," *AIChE J.*, **34**(6), 1043 (1988).

Miyahara, T., K. Tsuchiya, and L.-S. Fan, "Wake Properties of a Single Gas Bubble in a Three-Dimensional Liquid-Solid Fluidized Bed," *Int. J. Multiphase Flow*, **14**, 749 (1988).

Muroyama, K., M. Fukuma, and A. Yasunishi, "Wall-to-Bed Heat Transfer Coefficient in Gas-Liquid-Solid Fluidized Beds," *Can. J. Chem. Eng.*, **62**, 199 (1984).

Muroyama, K., M. Fukuma, and A. Yasunishi, "Wall-to-Bed Heat Transfer in Liquid-Solid and Gas-Liquid-Solid Fluidized Beds: II. Gas-Liquid-Solid Fluidized Beds," *Can. J. Chem. Eng.*, **64**, 409 (1986).

Ostergard, K., "Fluidization," *Soc. Chem. Ind., London*, 58 (1964).

Raghunathan, K., S. Kumar, and L.-S. Fan, "Pressure Distribution and Vortical Structure in the Wake Behind Gas Bubbles in Liquid and Liquid-Solid Systems," *Int. J. Multiphase Flow*, **18**, 41 (1992).

Suh, I. S., G. T. Jin, and S. D. Kim, "Heat-Transfer Coefficients in Three-Phase Fluidized Beds," *Int. J. Multiphase Flow*, **11**, 255 (1985).

Suh, I.-S., and W.-D. Deckwer, "Unified Correlation of Heat Transfer Coefficients in Three-Phase Fluidized Beds," *Chem. Eng. Sci.*, **44**, 1455 (1989).

Viswanathan, S., A. S. Kakar, and P. S. Murti, "Effect of Dispersed Bubbles into Liquid Fluidized Beds with Gas-Liquid Cocurrent Upflow," *Chem. Eng. Sci.*, 903 (1964).

Wasan, D. T., and M. S. Ahluwalia, "Consecutive Film and Surface Renewal Mechanism for Heat or Mass Transfer from a Wall," *Chem. Eng. Sci.*, **24**, 1535 (1969).

Manuscript received Dec. 27, 1991.